

Cite this: *Chem. Sci.*, 2022, 13, 12533

All publication charges for this article have been paid for by the Royal Society of Chemistry

A bis-NHC–CAAC dimer derived dicationic diradical^{†‡}

Mithilesh Kumar Nayak,^a Pallavi Sarkar,^b Benedict J. Elvers,^c Sakshi Mehta,^d Fangyuan Zhang,^e Nicolas Chrysochos,^a Ivo Krummenacher,^f Thangavel Vijayakanth,^g Ramakirushnan Suriya Narayanan,^a Ramapada Dolai,^a Biswarup Roy,^a Vishal Malik,^a Hemant Rawat,^h Abhishake Mondal,^{i,*d} Ramamoorthy Boomishankar,^{i,*g} Swapan K. Pati,^{i,*b} Holger Braunschweig,^{i,*f} Carola Schulzke,^{i,*c} Prince Ravat^{i,*e} and Anukul Jana^{i,*a}

The isolation of carbon-centered diradicals is always challenging due to synthetic difficulties and their limited stability. Herein we report the synthesis of a *trans*-1,4-cyclohexylene bridged bis-NHC–CAAC dimer derived thermally stable dicationic diradical. The diradical character of this compound was confirmed by EPR spectroscopy. The variable temperature EPR study suggests the singlet state to be marginally more stable than the triplet state ($2J = -5.5 \text{ cm}^{-1}$ ($\Delta E_{ST} = 0.065 \text{ kJ mol}^{-1}$)). The presence of the *trans*-1,4-cyclohexylene bridge is instrumental for the successful isolation of this dicationic diradical. Notably, in the case of ethylene or propylene bridged bis-NHC–CAAC dimers, the corresponding dicationic diradicals are transient and rearrange to hydrogen abstracted products.

Received 14th July 2022
Accepted 21st September 2022

DOI: 10.1039/d2sc03937k

rsc.li/chemical-science

Introduction

Diradical compounds are of quite substantial scientific importance due to their versatile applications in various research fields, ranging from synthetic chemistry to modern chemical physics.¹ In comparison to carbon-centered diradicals, the heteroatom-centered diradicals with unpaired electrons residing on nitrogen or oxygen centres are quite well studied.²

This is due to the fact that carbon-centered diradicals are generally much less stable.^{3,4} The design of synthetic pathways and the subsequent successful isolation of carbon-centered diradicals are therefore always challenging. Strategically, the synthesis of carbon-centered diradicals can be facilitated by applying electron transfer processes to redox-active organic molecules. In recent years, several such compounds have moved into the focus of interest: among them the electron donor tetrathiafulvalene (TTF) **I**⁵ and the electron acceptor *N,N'*-dimethyl-4,4'-bipyridinium dication (BIPY) **II**⁶ are of particular interest (Scheme 1). These comprehensively studied species **I** and **II** exhibit two reversible one-electron redox processes each and exist in three isolable oxidation states. Considering this kind of redox property, the synthesis of dicationic biradicals/diradicals involving two units of TTF as well as BIPY have been known such as **III**⁷ and **IV**.⁸ Moreover, compounds based on two or more TTF and/or BIPY units were intensely investigated for properties based on this notable redox-activity and for various applications including those as organic semiconductors, electrochromic devices, and molecular machines.⁹

Electronically related to TTF, in recent years several carbene-based electron-rich alkenes have been synthesized,^{10–14} such as the NHC–CAAC dimer **V**¹¹ (Scheme 1). These compounds exhibit two reversible one-electron redox processes and all three oxidation states can be isolated: neutral, radical cation, and dication, similar to **I** and **II**. In the case of the radical cation derived from NHC–CAAC dimers, the respective spin density resides mostly on the carbenic carbon of the CAAC-scaffolds.¹⁰ In recent years CAAC-scaffolds have become known to stabilize

^aTata Institute of Fundamental Research Hyderabad, Gopanally, Hyderabad-500107, India. E-mail: ajana@tifrh.res.in

^bTheoretical Sciences Unit, Jawaharlal Nehru Centre for Advanced Scientific Research, Bangalore-560064, India. E-mail: pati@jncasr.ac.in

^cInstitut für Biochemie, Universität Greifswald, Felix-Hausdorff-Straße 4, D-17489, Greifswald, Germany. E-mail: h.braunschweig@uni-greifswald.de

^dSolid State and Structural Chemistry Unit, Indian Institute of Science, Bangalore, 560012, India. E-mail: mondal@iisc.ac.in

^eInstitute of Organic Chemistry, University of Würzburg, Am Hubland, 97074 Würzburg, Germany. E-mail: princekumar.ravat@uni-wuerzburg.de

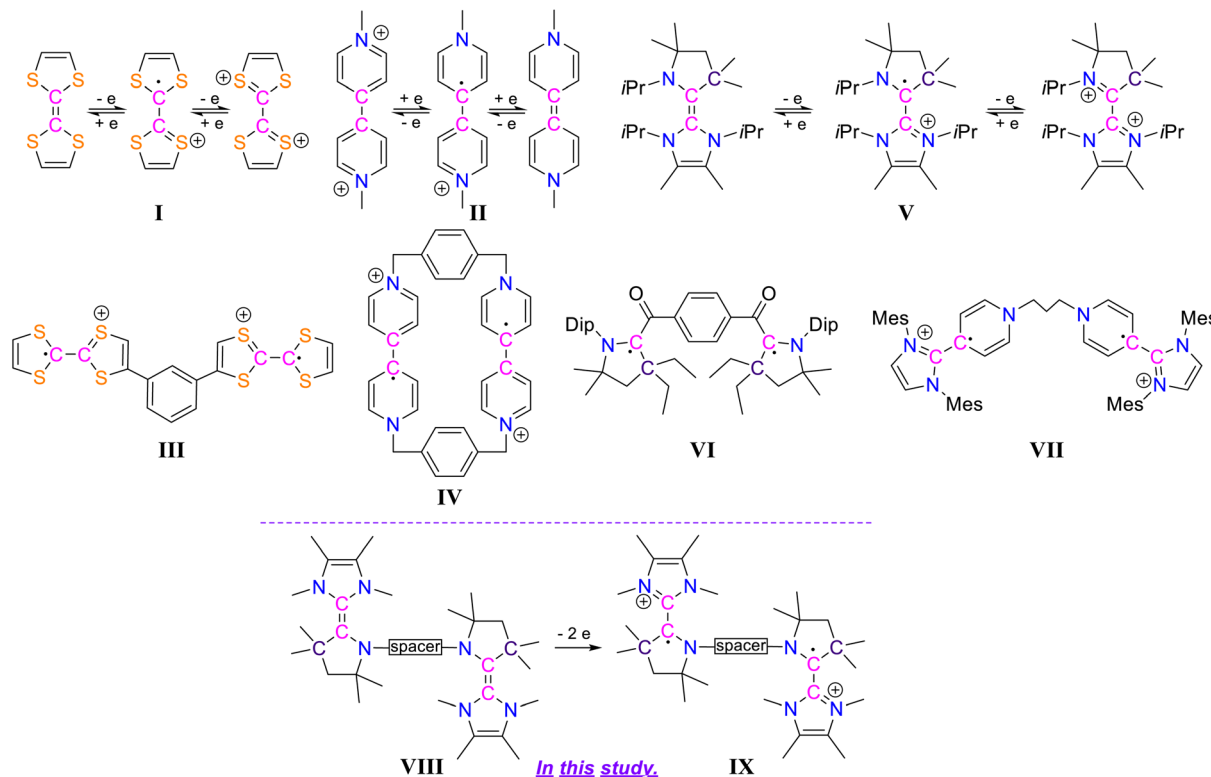
^fInstitute of Inorganic Chemistry and Institute for Sustainable Chemistry & Catalysis with Boron, Julius-Maximilians-Universität Würzburg, Am Hubland, 97074 Würzburg, Germany. E-mail: h.braunschweig@uni-wuerzburg.de

^gDepartment of Chemistry, Indian Institute of Science Education and Research Pune, Dr Homi Bhabha Road, Pune 411008, India. E-mail: boomi@iiserpune.ac.in

[†] Dedicated to Professor Sriram Ramaswamy on the occasion of his 65th birthday.

[‡] Electronic supplementary information (ESI) available: Experimental details, analytical data, NMR spectra, UV/Vis spectra, X-ray crystallographic details and details of theoretical calculation. CCDC 2047110 (**3**^{Et}), 2047111 (**4**^{Et}), 2047113 (**10**^{Et}), 2047114 (**5**^{Et}), 2047112 (**8**^{Et}), 2047115 (**9**^{Et}), 2161952 (**3**^{Pr}), 2161953 (**4**^{Pr}), 2161955 (**9**^{Pr}), 2161956 (**3**^{Cy}), 2161957 (**5**^{Cy}), 2161958 (**6**^{Cy}), 2161959 (**7**^{Cy}), 2204009 (**5**^{Pr}). For ESI and crystallographic data in CIF or other electronic format see <https://doi.org/10.1039/d2sc03937k>





Scheme 1 Chemical structures of I–IX.

various carbon-centered based open-shell compounds.¹⁵ Among them the isolation of biradical **VI**¹⁶ (Scheme 1) demonstrates the potential of CAAC-scaffolds to act as paramagnetic building blocks. Also there was a report of pyridinium–NHC derived diradical **VII** (Scheme 1).¹³ Thinking strategically, the generation of radical cation based biradicals/diradicals should, hence, be possible by developing a new class of compounds bearing two NHC–CAAC dimer motifs, *i.e.* species **VIII** (Scheme 1).

Herein we report the synthesis of the *trans*-1,4-cyclohexylene bridged bis-NHC–CAAC dimer **VIII** derived dicationic diradical **IX** (Scheme 1). The presence of the *trans*-1,4-cyclohexylene bridge, which is tethered to the N-atoms of the two CAAC scaffolds, is crucial for the successful isolation of the dicationic diradical. In the case of an ethylene or a propylene bridge being used for the bis-NHC–CAAC dimers, their dicationic diradicals were only transiently formed and rearranged to the hydrogen abstracted products.

Results and discussion

First, in order to obtain the *trans*-1,4-cyclohexylene bridged bis-NHC–CAAC dimer, **1**^{Cy} was reacted with **2**¹⁷ giving **3**^{Cy} in a 90% yield (Scheme 2).¹⁸ The reaction proceeds either through the nucleophilic addition of NHC to the pyrrolinium cation or acid–base reaction under the formation of bis-CAAC followed by C–H insertion.^{13,19} Recently, a related bis-CAAC with *trans*-1,4-cyclohexylene framework was reported.²⁰ The subsequent reaction of **3**^{Cy} with two equivalents of LDA leads to the formation of the

light yellow colored bis-NHC–CAAC dimer **4**^{Cy} in a 83% yield (Scheme 2).¹⁸ Compound **4**^{Cy} is inherently prone to undergo a four-electron oxidation, which was, consequently, tested. The reaction with four equivalents of AgOTf leads to the formation of the tetracation **5**^{Cy} in a 89% yield and this redox transition is reversible (Scheme 2).¹⁸ Subsequently, the 1 : 1 reaction of **4**^{Cy} with **5**^{Cy} yielded thermally stable **6**^{Cy} as a dark red crystalline solid almost quantitatively. We also observed the formation of **6**^{Cy} from the reaction of **4**^{Cy} with two equivalents of AgOTf, but the associated purification step is essentially unmanageable. Formation of **6**^{Cy} was confirmed by its solid-state molecular structure determination (Fig. 1). The C2–C3/C5–C6 bond lengths between the NHC and CAAC moieties of **6**^{Cy} are 1.439(7)/1.431(7) Å, *i.e.* close to the related radical cation of the NHC–CAAC dimer **V** (1.444 Å) and longer than that of the neutral species **V** (1.358 Å).¹¹

The spin density plot of **6**^{Cy} places the maximum spin density on the carbenic carbon atoms of the CAAC-scaffolds (Fig. S109[†]). In the UV/Vis spectrum, compound **6**^{Cy} exhibits the longest wavelength absorbance at $\lambda_{\text{max}} = 455$ nm. TD-DFT calculations suggest that the lowest-energy absorbance band arises mainly from the HOMO- $\alpha \rightarrow$ LUMO- $\alpha + 1$ transition, while the HOMO- $\alpha \rightarrow$ LUMO- α and HOMO- $\beta \rightarrow$ LUMO- β transitions exhibit very weak oscillator strengths (Fig. S108 and Table S17[†]).

EPR spectroscopy of **6**^{Cy} in frozen 1 : 1 toluene/acetonitrile solution confirmed its diradical nature with a weak half-field signal (Fig. 2 – left), which is readily detectable in the



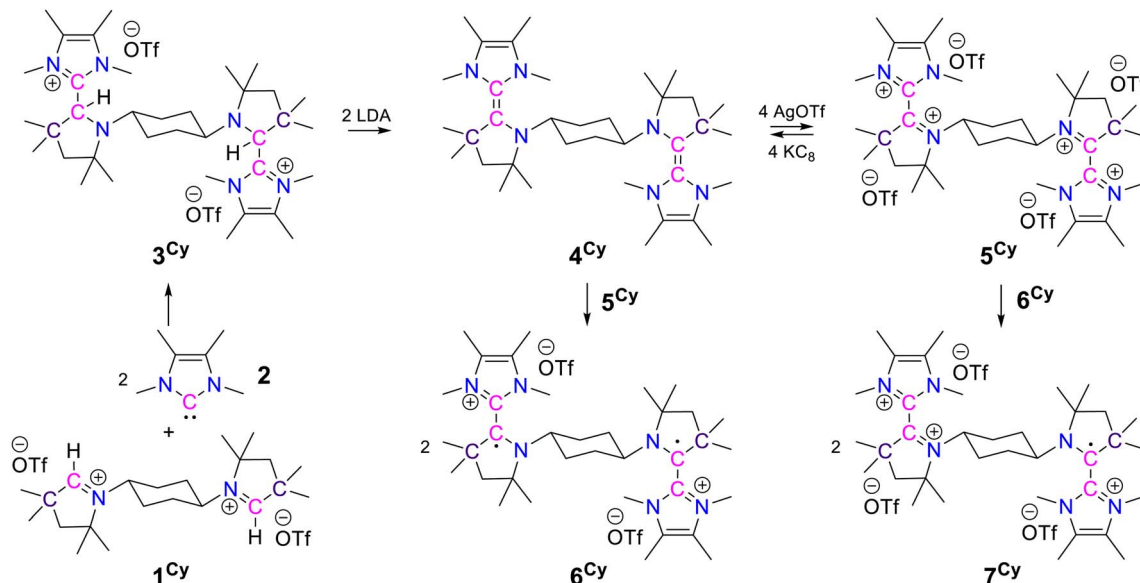
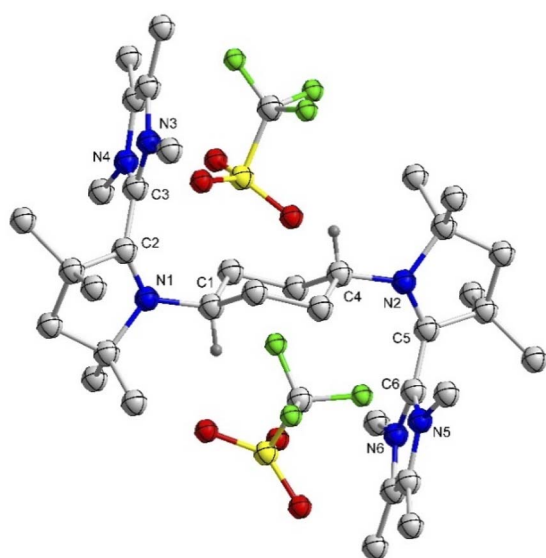
Scheme 2 Synthesis of 3^{Cy} , 4^{Cy} , 5^{Cy} , 6^{Cy} , and 7^{Cy} .

Fig. 1 Molecular structure of 6^{Cy} in the solid state with thermal ellipsoids at the 50% probability level. All hydrogen atoms except on C1 and C4 are omitted for clarity. Selected bond lengths (Å) and bond angles ($^{\circ}$): N1–C2 1.380(6), C2–C3 1.439(7), N2–C5 1.366(6), C5–C6 1.431(7); N1–C2–C3 122.3(4), N2–C5–C6 122.5(4).

temperature range of 10 to 140 K (Fig. 2 – middle). Fitting of the temperature-dependent double-integral intensity to the Bleaney-Bowers model gives a small singlet-triplet gap of $2J = -5.5 \text{ cm}^{-1}$ ($\Delta E_{\text{ST}} = 0.065 \text{ kJ mol}^{-1}$) (Fig. S83 \ddagger). Similarly, weak exchange couplings were also observed for diradicals III,⁷ VI,¹⁶ and VII.¹³ The small singlet-triplet energy gap was confirmed by a SQUID magnetometer measurement of 6^{Cy} as the high-temperature Curie Weiss fitting provides a Weiss constant of $\theta = -3.065 \text{ K}$, corresponding to an energy gap of $0.025 \text{ kJ mol}^{-1}$ (Fig. S88 \ddagger). Using the relative intensity of the half-field ($\Delta M_s =$

± 2) to the allowed transitions ($\Delta M_s = \pm 1$), the distance r between the unpaired spins can be estimated to be *ca.* 8.8 \AA ,²¹ relatively similar, hence, to the distances between the two carbonic carbon atoms of CAAC-scaffolds in 6^{Cy} (7.364 \AA).

Quantum chemical calculations were performed to verify the nature of the ground state and estimate the energy gap between the singlet and triplet states of 6^{Cy} . Initially, the energies of singlet and triplet states were calculated by DFT using four different functionals ωB97XD , MN12SX, B3LYP-D3, and PBE0 with the Def2SVP basis-set (Table S16 \ddagger). Calculations provided values of ΔE_{ST} in the range of -0.015 to 0.10 kJ mol^{-1} , which is in accordance with the small ΔE_{ST} obtained from EPR experiments. The negative value of the exchange coupling constant J from EPR studies indicates antiferromagnetic coupling between two-spin centers and, hence, a singlet ground state. Interestingly, while the ωB97XD functional gave a positive value for J , MN12SX, B3LYP-D3, and PBE0 yielded negative values corroborating the EPR results. This may be based on the fact that the ΔE_{ST} is very small. Multi-reference theoretical methods are known to precisely describe the energies of singlet and triplet states. Indeed the multi-reference CASSCF(2,2)/NEVPT2/def2-TZVP approach²² verified the singlet ground states and provided a much more accurate adiabatic ΔE_{ST} of $-0.037 \text{ kJ mol}^{-1}$.

Subsequently, we have synthesized the radical-trication 7^{Cy} by the 1 : 1 reaction of 5^{Cy} with 6^{Cy} in a 88% yield (Scheme 2).¹⁸ The comproportionation reaction between 6^{Cy} and 5^{Cy} gives rise to an EPR signal centered around $g = 2.0029$, indicating the formation of radical-trication 7^{Cy} (Fig. 2 – right). The single crystal X-ray structural analysis (Fig. 3) identifies two different C–C bond lengths between the NHC and CAAC moieties C2–C3 $1.459(4)$ /C5–C6 $1.488(4) \text{ \AA}$, which suggests that one NHC–CAAC unit is oxidized twice and the other one is oxidized only once. This is further supported by the C–N bond distances of the two CAAC-scaffolds (C2–N1 $1.361(4)$ /C5–N2 $1.277(3) \text{ \AA}$).



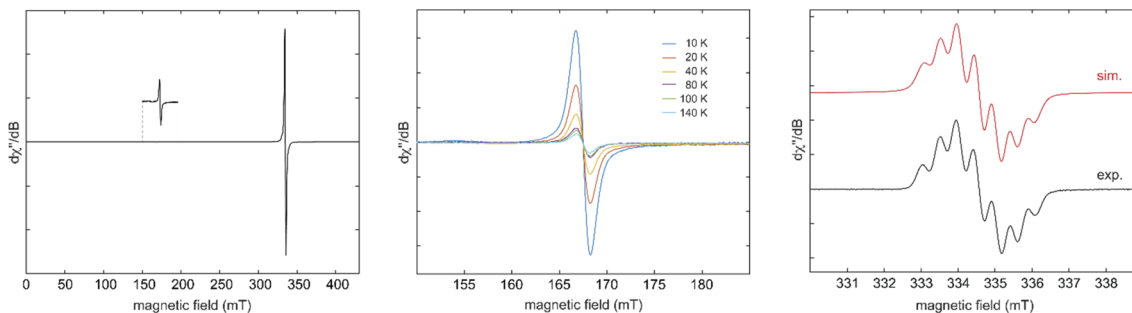


Fig. 2 CW EPR spectrum of 6^{Cy} in a 1 : 1 toluene/acetonitrile mixture at 40 K (left), temperature dependence of the half-field transitions between 10 and 140 K (middle), and experimental (black) and simulated (red) EPR spectra of 7^{Cy} in acetonitrile (right). Best-fit simulation parameters: $g_{\text{iso}} = 2.0029$, $a(^{14}\text{N}) = 14.2$ MHz (1N), 11.8 MHz (2N), and $a(^1\text{H}) = 3.2$ MHz (6H).

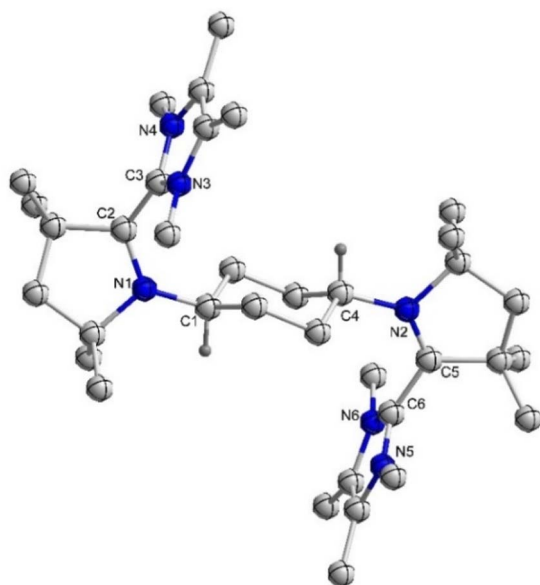
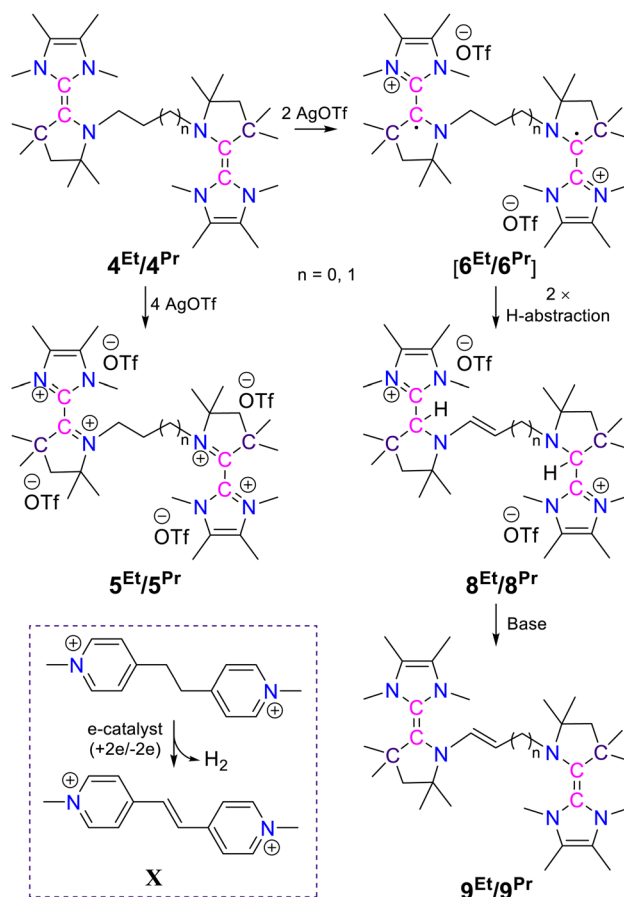


Fig. 3 Molecular structure of 7^{Cy} in the solid state with thermal ellipsoids at the 50% probability level. All hydrogen atoms except on C1 and C4 and three triflate anions are omitted for clarity. Selected bond lengths (Å) and bond angles ($^\circ$): N1–C2 1.361(4), C2–C3 1.459(4), N2–C5 1.277(3), C5–C6 1.488(4); N1–C2–C3 122.0(3), N2–C5–C6 125.2(2).

To address the influence of the alkylene bridge, which is tethered to the N-atoms of the CAAC scaffolds, we have also synthesized and studied the ethylene and the propylene bridged bis-NHC–CAAC dimers $4^{\text{Et}}/4^{\text{Pr}}$. Both of these bis-NHC–CAAC dimers $4^{\text{Et}}/4^{\text{Pr}}$ undergo four-electron oxidation with AgOTf under the formation of $5^{\text{Et}}/5^{\text{Pr}}$ in good yields ($5^{\text{Et}} = 76\%$ and $5^{\text{Pr}} = 89\%$) (Scheme 3).¹⁸ However, in contrast to *trans*-1,4-cyclohexylene bridged 4^{Cy} , the ethylene/propylene bridged bis-NHC–CAAC dimers $4^{\text{Et}}/4^{\text{Pr}}$ upon two-electron oxidation do not facilitate the isolation of bis-radical cations $6^{\text{Et}}/6^{\text{Pr}}$. Instead these transient species proceed to double H-abstraction²³ under the formation of ethenylene/propenylene-bridged dication $8^{\text{Et}}/8^{\text{Pr}}$ (Scheme 3).¹⁸ The formation of $8^{\text{Et}}/8^{\text{Pr}}$ was also realized by the 1 : 1 reaction of $4^{\text{Et}}/4^{\text{Pr}}$ and $5^{\text{Et}}/5^{\text{Pr}}$. Moreover, the formation of 8^{Et} has been confirmed by the solid-state molecular structure

determination (Fig. 4). Compound 8^{Et} can be classified as disubstituted *E*-diamino alkene and exhibits electron-rich nature. Its oxidation with AgOTf leads to the partial formation of corresponding radical trication, which has been confirmed by solid-state structure determination (Fig. S77[†]) and EPR spectroscopy (Fig. S87[†]). Quantitative EPR measurement indicates a radical concentration of *ca.* 54% in the crystalline crude products considering TEMPO as standard.



Scheme 3 Synthesis of $5^{\text{Et}}/5^{\text{Pr}}$, $8^{\text{Et}}/8^{\text{Pr}}$, and $9^{\text{Et}}/9^{\text{Pr}}$ (Insert: Schematic Presentation of X).



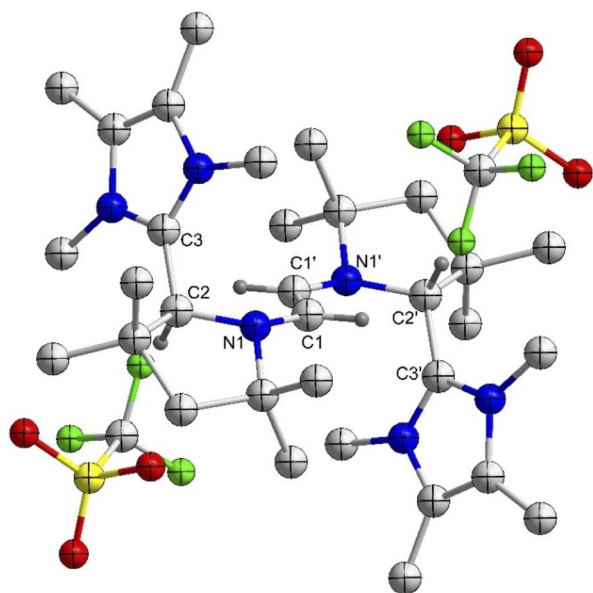


Fig. 4 Molecular structure of 8^{Et} in the solid state with thermal ellipsoids at the 50% probability level. All hydrogen atoms except on C1, C1', C2, and C2' are omitted for clarity. Selected bond lengths (Å) and bond angles ($^{\circ}$): N1–C2 1.457(2), C2–C3 1.505(3), C1–C1' 1.324 (4); N1–C2–C3 111.82(15), N1–C1–C1' 127.4(3).

These observations confirm the formation of bis-radical cation intermediates $6^{\text{Et}}/6^{\text{Pr}}$ which have very limited stability compared to 6^{Cy} , emphasizing the critically important influence of the alkylene bridge. In case of the ethylene/propylene bridge, most likely the facile C–C double bond formation after the double H-abstraction is responsible for the limited stability of their dicationic diradicals. Such type of facile C–C double bond formation at the *trans*-1,4-cyclohexylene bridge is impaired by conformational restriction. As a result, the *trans*-1,4-cyclohexylene bridge is instrumental in stabilizing the dicationic diradical.

These newly synthesized bis-NHC–CAAC dimers 4^{Cy} , 4^{Et} , and 4^{Pr} react with ($[n\text{Bu}_4\text{N}][\text{PF}_6]$) (Fig. S6 \ddagger) and therefore we were not able to obtain cyclic voltammetric results. Subsequently, we carried out the cyclic voltammetric studies of the corresponding tetracations 5^{Cy} , 5^{Et} , and 5^{Pr} along with dicationic diradical 6^{Cy} and radical tri-cation 7^{Cy} in acetonitrile (0.1 M $[n\text{Bu}_4\text{N}][\text{PF}_6]$). Compound 5^{Cy} exhibits two cathodic reversible waves at $E_{\text{pk}} = -1.07$ V (with a shoulder at $E_{\text{pk}} = -0.95$ V) and $E_{\text{pk}} = -1.66$ V (at 100 mV s^{-1} scan rate) likely associated with the formation of dicationic diradical 6^{Cy} and bis-NHC–CAAC dimer 7^{Cy} (Fig. 5). The first cathodic wave is closely associated with two one-electron reduction processes and the second cathodic wave is for a two-electron reduction process, which was confirmed by a differential pulse voltammetry (DPV) study (Fig. S93 \ddagger). Considering the relative current height of the backward oxidation process from the measurements at 100 mV s^{-1} and 1000 mV s^{-1} scan rates, confirms the instability of the generated bis-alkene towards the electrolyte $[n\text{Bu}_4\text{N}][\text{PF}_6]$. The cyclic voltammetric studies of 6^{Cy} and 7^{Cy} exhibit the redox processes as expected and along the line of 5^{Cy} (Fig. S94–S99 \ddagger). On the other

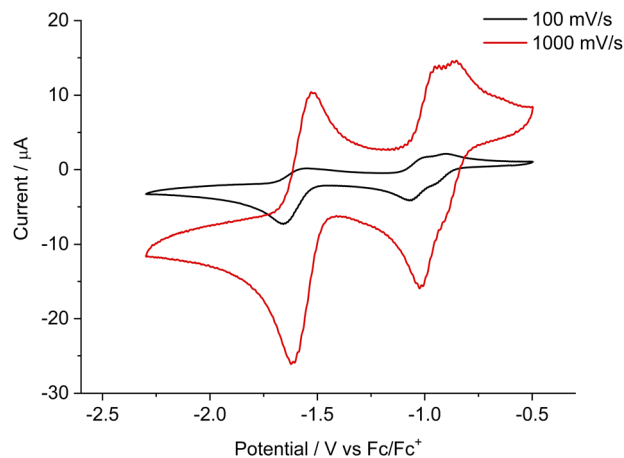


Fig. 5 Cyclic voltammetry plots for 5^{Cy} at a scan rate of 100 mV s^{-1} and 1000 mV s^{-1} in acetonitrile (0.1 M $[n\text{Bu}_4\text{N}][\text{PF}_6]$).

hand, the scan rate dependent cyclic voltammetry along with differential pulse voltammetry (DPV) studies of 5^{Et} and 5^{Pr} indicate that follow up chemical reactions occurred after the two-electron reduction (Fig. S100–S107 \ddagger) which is in accordance with the chemical reduction experiments. The first reduction event in both cases 5^{Et} and 5^{Pr} is reversible, though (Fig. S102 \ddagger).

Lastly it was shown that $8^{\text{Et}}/8^{\text{Pr}}$ can be converted to the crystalline *N,N'*-ethenylene/propenylene-bridged bis-NHC–CAAC dimers $9^{\text{Et}}/9^{\text{Pr}}$ by double deprotonation reactions (Scheme 3).¹⁸ The formation of *N,N'*-ethenylene/propenylene-bridged bis-NHC–CAAC dimers $9^{\text{Et}}/9^{\text{Pr}}$ have been unambiguously confirmed by their solid state molecular structure determination (Fig. S76 \ddagger and 6). The overall transformation of the *N,N'*-ethenylene/propylene-bridged bis-NHC–CAAC dimers $4^{\text{Et}}/4^{\text{Pr}}$

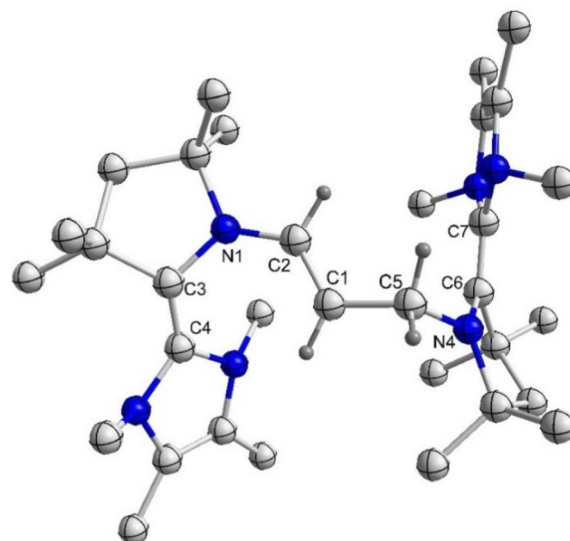


Fig. 6 Molecular structure of 9^{Pr} in the solid state with thermal ellipsoids at the 50% probability level. All hydrogen atoms except on C2, C1, and C5 are omitted for clarity. Selected bond lengths (Å) and bond angles ($^{\circ}$): N1–C3 1.4200(18), C3–C4 1.352(2), C1–C2 1.330(2); N1–C3–C4 122.66(12), N1–C2–C1 129.63(14).



into the *N,N'*-ethenylene/propenylene-bridged bis-NHC–CAAC dimers $9^{\text{Et}}/9^{\text{Pr}}$ is notably reminiscent of the recently reported electron-catalyzed dehydrogenation of a saturated bipyridinium-ethane backbone to a conjugated bipyridinium-ethene backbone **X** by Stoddart *et al.* (Scheme 3 – insert).²³

Conclusions

In conclusion, we have synthesized a *trans*-1,4-cyclohexylene-bridged bis-NHC–CAAC dimer derived radical-cation based crystalline and thermally stable diradical. Its singlet state is only marginally more stable than the triplet state ($2J = -5.5 \text{ cm}^{-1}$ ($\Delta E_{\text{ST}} = 0.065 \text{ kJ mol}^{-1}$)). The related radical-trication and the tetra-cation were also isolated and characterized. Importantly, this study points to the choice of the alkylene bridge being crucial for the stabilization and successful isolation of the dicationic diradical. With ethylene/propylene bridged bis-NHC–CAAC dimers, the corresponding dicationic diradicals are transient and rearrange to the hydrogen abstracted products. The latter can be converted to ethenylene and propenylene-bridged bis-NHC–CAAC dimers; these transformations constitute dehydrogenations of the alkylene bridges. Notably, with this synthetic route an extensive substrate scope can be realized both in the NHC and CAAC scaffolds as well as in the bridging unit.

Data availability

Full experimental and computational details are provided as part of the ESI.†

Author contributions

M. K. N. lead all the synthesis and characterization along with initial contribution from R. D., B. R. and V. M., P. S., S. K. P. and P. R. performed the theoretical calculations. T. V., R. S. N., H. R., R. B. and C. S. for the single crystal XRD study. I. K. and H. B. for EPR study. S. M. and A. M. for SQUID study. B. J. E., F. Z., N. C., C. S. and P. R. for electrochemistry study. M. K. N. and A. J. designed the research work. M. K. N. and A. J. prepared the ESI.† A. J. wrote the manuscript and all authors assisted in writing and editing the manuscript. A. J. supervised the study.

Conflicts of interest

There are no conflicts to declare.

Acknowledgements

We acknowledge generous support of the Department of Atomic Energy, Government of India, under Project Identification No. RTI 4007 and SERB (CRG/2019/003415), India. The National Facility for High-Field NMR, TIFR-Hyderabad, is highly acknowledged. AM thanks the Council of Scientific and Industrial Research (CSIR), Govt. of India (Project No: 01(3031)/21/EMR-II), and the Solid State and Structural Chemistry Unit at the Indian Institute of Science (IISc) Bangalore, India, for

providing the SQUID Magnetometer facility. We thank the reviewers for their insightful comments helping to improve the quality of the manuscript. AJ is very much grateful to the Alexander von Humboldt Foundation for the sponsoring of a renewed research stay.

Notes and references

- (a) M. Abe, *Chem. Rev.*, 2013, **113**, 7011–7088; (b) T. Stuyver, B. Chen, T. Zeng, P. Geerlings, F. D. Proft and R. Hoffmann, *Chem. Rev.*, 2019, **119**, 11291–11351.
- (a) S. Zhang, M. Pink, T. Junghoefer, W. Zhao, S. N. Hsu, S. Rajca, A. Calzolari, B. W. Boudouris, M. B. Casu and A. Rajca, *J. Am. Chem. Soc.*, 2022, **144**, 6059–6070; (b) N. Gallagher, H. Zhang, T. Junghoefer, E. Giangrisostomi, R. Ovsyannikov, M. Pink, S. Rajca, M. B. Casu and A. Rajca, *J. Am. Chem. Soc.*, 2019, **141**, 4764–4774; (c) A. Rajca, A. Olankitwanit and S. Rajca, *J. Am. Chem. Soc.*, 2011, **133**, 4750–4753; (d) W. T. Borden, R. Hoffmann, T. Stuyver and B. Chen, *J. Am. Chem. Soc.*, 2017, **139**, 9010–9018; (e) H. Han, D. Zhang, Z. Zhu, R. Wei, X. Xiao, X. Wang, Y. Liu, Y. Ma and D. Zhao, *J. Am. Chem. Soc.*, 2021, **143**, 17690–17700; (f) S. Arikawa, A. Shimizu, D. Shiomi, K. Sato and R. Shintani, *J. Am. Chem. Soc.*, 2021, **143**, 19599–19605.
- (a) A. Rajca, S. Utamapanya and J. Xu, *J. Am. Chem. Soc.*, 1991, **113**, 9235–9241; (b) C. Shu, H. Zhang, A. Olankitwanit, S. Rajca and A. Rajca, *J. Am. Chem. Soc.*, 2019, **141**, 17287–17294; (c) D. Schmidt, M. Son, J. M. Lim, M. J. Lin, I. Krummenacher, H. Braunschweig, D. Kim and F. Würthner, *Angew. Chem., Int. Ed.*, 2015, **54**, 13980–13984; (d) A. Rajca, K. Shiraishia and S. Rajca, *Chem. Commun.*, 2009, 4372–4374.
- (a) A. Jana, M. Ishida, J. S. Park, S. Bähring, J. O. Jeppesen and J. L. Sessler, *Chem. Rev.*, 2017, **117**, 2641–2710; (b) H. V. Schröder and C. A. Schalley, *Beilstein J. Org. Chem.*, 2018, **14**, 2163–2185; (c) N. Duvva, U. Chilakamarthi and L. Giribabu, *Sustainable Energy Fuels*, 2017, **1**, 678–688.
- (a) L. Striepe and T. Baumgartner, *Chem.–Eur. J.*, 2017, **23**, 16924–16940; (b) M. Berville, J. Richard, M. Stolar, S. Choua, N. Le Breton, C. Gourlaouen, C. Boudon, L. Ruhlmann, T. Baumgartner, J. A. Wytko and J. Weiss, *Org. Lett.*, 2018, **20**, 8004–8008; (c) T. Nakazato, H. Takekoshi, T. Sakurai, H. Shinokubo and Y. Miyake, *Angew. Chem., Int. Ed.*, 2021, **60**, 13877–13881.
- F. Riobé, N. Avarvari, P. Grosshans, H. Sidorenkova, T. Berclazb and M. Geoffroy, *Phys. Chem. Chem. Phys.*, 2010, **12**, 9650–9660.
- M. Frascioni, I. R. Fernando, Y. Wu, Z. Liu, W.-G. Liu, S. M. Dyar, G. Barin, M. R. Wasielewski, W. A. Goddard III and J. Fraser Stoddart, *J. Am. Chem. Soc.*, 2015, **137**, 11057–11068.
- (a) J. Jung, W. Liu, S. Kim and D. Lee, *J. Org. Chem.*, 2019, **84**, 6258–6269; (b) A. Jana, S. Bähring, M. Ishida, S. Goeb, D. Canevet, M. Salle, J. O. Jeppesen and J. L. Sessler, *Chem. Soc. Rev.*, 2018, **47**, 5614–5645; (c) J. F. Stoddart, *Angew. Chem., Int. Ed.*, 2017, **56**, 11094–11125; (d) Y. Wang,



- M. Frascioni and J. F. Stoddart, *ACS Cent. Sci.*, 2017, **3**, 927–935.
- 9 D. Munz, J. Chu, M. Melaimi and G. Bertrand, *Angew. Chem., Int. Ed.*, 2016, **55**, 12886–12890.
- 10 (a) D. Mandal, R. Dolai, R. Kumar, S. Suhr, N. Chrysochos, P. Kalita, R. S. Narayanan, G. Rajaraman, C. Schulzke, B. Sarkar, V. Chandrasekhar and A. Jana, *Org. Lett.*, 2017, **19**, 5605–5608; (b) D. Mandal, R. Dolai, N. Chrysochos, P. Kalita, R. Kumar, D. Dhara, A. Maiti, R. S. Narayanan, G. Rajaraman, C. Schulzke, V. Chandrasekhar and A. Jana, *J. Org. Chem.*, 2019, **84**, 8899–8909; (c) D. Mandal, F. Stein, S. Chandra, N. I. Neuman, P. Sarkar, S. Das, A. Kundu, A. Sarkar, H. Rawat, S. K. Pati, V. Chandrasekhar, B. Sarkar and A. Jana, *Chem. Commun.*, 2020, **56**, 8233–8236; (d) M. K. Nayak, S. Suhr, N. Chrysochos, H. Rawat, C. Schulzke, V. Chandrasekhar, B. Sarkar and A. Jana, *Chem. Commun.*, 2021, **57**, 1210–1213; *Chem. Commun.*, 2021, **57**, 4979–4980.
- 11 U. S. D. Paul and U. Radius, *Chem.–Eur. J.*, 2017, **23**, 3993–4009.
- 12 (a) P. W. Antoni and M. M. Hansmann, *J. Am. Chem. Soc.*, 2018, **140**, 14823–14835; (b) P. W. Antoni, T. Bruckhoff and M. M. Hansmann, *J. Am. Chem. Soc.*, 2019, **141**, 9701–9711; (c) P. W. Antoni, C. Golz and M. M. Hansmann, *Angew. Chem., Int. Ed.*, 2022, **61**, e202203064.
- 13 J. Messelberger, A. Grünwald, S. J. Goodner, F. Zeilinger, P. Pinter, M. E. Miehllich, F. W. Heinemann, M. M. Hansmann and D. Munz, *Chem. Sci.*, 2020, **11**, 4138–4149.
- 14 (a) M. Melaimi, R. Jazzar, M. Soleilhavoup and G. Bertrand, *Angew. Chem., Int. Ed.*, 2017, **56**, 10046–10068; (b) M. Soleilhavoup and G. Bertrand, *Acc. Chem. Res.*, 2015, **48**, 256–266; (c) S. Kundu, S. Sinhababu, V. Chandrasekhar and H. W. Roesky, *Chem. Sci.*, 2019, **10**, 4727–4741; (d) J. K. Mahoney, D. Martin, F. Thomas, C. E. Moore, A. L. Rheingold and G. Bertrand, *J. Am. Chem. Soc.*, 2015, **137**, 7519–7525; (e) M. M. Hansmann, M. Melaimi and G. Bertrand, *J. Am. Chem. Soc.*, 2017, **139**, 15620–15623; (f) D. Mandal, S. Sobottka, R. Dolai, A. Maiti, D. Dhara, P. Kalita, R. S. Narayanan, V. Chandrasekhar, B. Sarkar and A. Jana, *Chem. Sci.*, 2019, **10**, 4077–4081; (g) M. M. Hansmann, M. Melaimi and G. Bertrand, *J. Am. Chem. Soc.*, 2018, **140**, 2206–2213; (h) M. M. Hansmann, M. Melaimi, D. Munz and G. Bertrand, *J. Am. Chem. Soc.*, 2018, **140**, 2546–2554.
- 15 J. K. Mahoney, D. Martin, C. E. Moore, A. L. Rheingold and G. Bertrand, *J. Am. Chem. Soc.*, 2013, **135**, 18766–18769.
- 16 N. Kuhn and T. Kratz, *Synthesis*, 1993, 561–562.
- 17 See the ESI† for the experimental details, analytical data, NMR spectra, UV/Vis spectra, X-ray crystallographic details, and details of quantum chemical calculation.
- 18 (a) D. Mandal, R. Dolai, P. Kalita, R. S. Narayanan, R. Kumar, S. Sobottka, B. Sarkar, G. Rajaraman, V. Chandrasekhar and A. Jana, *Chem.–Eur. J.*, 2018, **24**, 12722–12727; (b) U. S. D. Paul and U. Radius, *Chem.–Eur. J.*, 2017, **23**, 3993–4009.
- 19 B. M. P. Lombardi, E. R. Pezoulas, R. A. Suvinen, A. Harrison, Z. S. Dubrawski, B. S. Gelfand, H. M. Tuononen and R. Roesler, *Chem. Commun.*, 2022, **58**, 6482–6485.
- 20 S. S. Eaton, K. M. More, B. M. Sawant and G. R. Eaton, *J. Am. Chem. Soc.*, 1983, **105**, 6560–6567.
- 21 Y. Guo, K. Sivalingam, E. F. Valeev and F. Neese, *J. Chem. Phys.*, 2017, **147**, 064110.
- 22 (a) M. K. Nayak, J. Stubbe, N. I. Neuman, R. S. Narayanan, S. Maji, C. Schulzke, V. Chandrasekhar, B. Sarkar and A. Jana, *Chem.–Eur. J.*, 2020, **26**, 4425–4431; (b) R. Kumar, S. Chandra, M. K. Nayak, A. S. Hazari, B. J. Elvers, C. Schulzke, B. Sarkar and A. Jana, *ACS Omega*, 2022, **7**, 837–843.
- 23 H. Chen, F. Jiang, C. Hu, Y. Jiao, S. Chen, Y. Qiu, P. Zhou, L. Zhang, K. Cai, B. Song, X. Y. Chen, X. Zhao, M. R. Wasielewski, H. Guo, W. Hong and J. F. Stoddart, *J. Am. Chem. Soc.*, 2021, **143**, 8476–8487.

